Automated Segmentation of the Optic Nerve Head for Glaucoma Diagnosis*

Radim Chrástek[1], Matthias Wolf[1], Klaus Donath[1], Heinrich Niemann[1], Torsten Hothorn[2], Berthold Lausen[2], Robert Lämmer[3], Christian Y. Mardin[3] and Georg Michelson[3]

[1]FORWISS, Knowledge Processing Research Group, 91058 Erlangen
[2]Department of Medical Informatics, Biometry and Epidemiology
[3]Department of Ophthalmology and Eye Hospital
Friedrich-Alexander-University, 91054 Erlangen
Email: chrastek@forwiss.de

Abstract. The diagnosis of glaucoma is closely associated with a morphological change in the optic nerve head (ONH), which can be examined with a scanning laser ophthalmoskop (Heidelberg Retina Tomograph). In this contribution a method for automated segmentation of the external margin of the ONH is presented. The method is based on morphological operations, Hough transform and Active Contours. The method was compared with a manually outlined margin on a subset of 159 subjects from the Erlangen Glaucoma Register. The correct classification rate was estimated to be 77.8% when using a tree-based classificator. This result is comparable with the estimated rate based on a manual outlining of the ONH.

1 Introduction

Glaucoma is the second most common cause of blindness worldwide. But it can be prevented if it is detected in its early stage. The diagnosis of glaucoma is closely associated with a morphological change in the optic nerve head (ONH) that can be examined with the Heidelberg Retina Tomograph (HRT). Shape parameters are calculated from the HRT mean topography images after manually outlining the contour line of the inner edge of Elschnig's scleral ring by an eye doctor into the HRT reflectivity image. This is not only time-consuming and subjective, this procedure also has a limited reproducibility. For that reason a method for automatic detection of the optic disc margin would be of great value. Furthermore it would provide the possibility to use the laser scanning tomography as tool in screening methods for glaucoma.

The HRT reflectivity image is first preprocessed in order to correct differences in illumination. Then, the rough position of the optic disc is estimated, a Region of Interest (ROI) is extracted, and the search space for the outer margin is restricted. In the last step, the estimated external border is smoothed by

* This work is funded by SFB 539, Project A 4. Only the authors are responsible for the contents

Fig. 1. Optic disc localisation. Thresholded image (a); Euclidian distance map (b); Valid regions (c); Detected center of the optic disc (d)

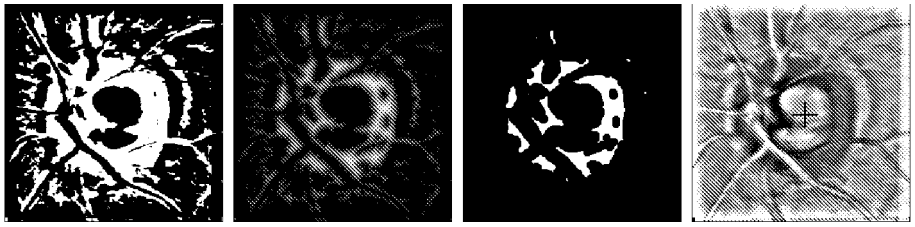

(a) (b) (c) (d)

means of Active Contours. The approach has been evaluated quantitatively and qualitatively.

2 Image Data and Preprocessing

Images of the patient's retina are acquired with confocal laser scanning microscopes *Heidelberg Retina Tomograph HRT I* and *HRT II*. Our method is applied to the reflectivity (intensity) images (size 256×256 pixel) with all possible fields of view (HRT I: $10° \times 10°$, $15° \times 15°$, $20° \times 20°$; HRT II: $15° \times 15°$).

Due to differences in illumination and contrast even an ophthalmologist can hardly recognize the outer optic disc margin correctly. Therefore, HRT images are preprocessed in order to normalize illumination and contrast (see [1]).

3 Segmentation of the Optic Disc

3.1 Optic Disc Localization

After correction of differences in illumination, the optic nerve head represents the darkest part in the image. Thus, the estimation of the optic nerve head corresponds with finding dark areas in the image. For this, the image is thresholded by θ_{ONH} which is automatically calculated based on mean gray value and standard deviation of all pixels (Fig. 1 (a)).

To remove noise and small regions an Euclidian Distance Map (EDM) is calculated that assignes each pixel the value of distance to the next region boundary (Fig. 1 (b)). After that the EDM is thresholded by removing all pixels with values lower than 5. In this way, all background artifacts and image pixels belonging to vessels are filtered out reliably (Fig. 1 (c)) and the center of gravity of the remaining pixels is assumed to be the rough position of the center of the optic disc, see Fig. 1 (d).

3.2 Estimation of the Optic Disc Margin

In the next processing steps different strategies are pursued to restrict the search space for the potential contour. Later, these restrictions are merged and the border of the optic nerve head is determined with respect to these constraints.

Fig. 2. Different search spaces/constraints. Rough restriction of the search space (a); Detected circular structure (b); Detected parapapillary athrophy (c); Possible valid contour points (d)

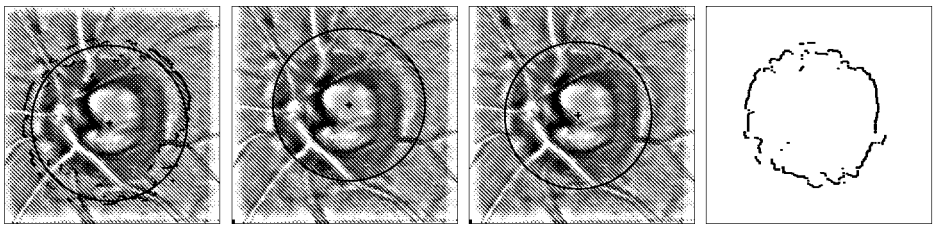

(a) (b) (c) (d)

Rough Restriction of the Search Space. The searched space is roughly restricted by a circle (see Fig. 2 (a)) fitted to optic disc margin candidates. The candidates are the most distant foreground pixels in the thresholed image (see Fig. 1 (a)) from the detected optic disc center in radial direction. The candidates are allowed within a certain radius only. The radius was set to 100 pixels for the field of view (fov) $10° \times 10°$, 70 pixels for the fov $15° \times 15°$and 55 pixels for the fov $20° \times 20°$.

Detection of Circular Structure. The optic disc margin has a nearly circular appearence. For this, the Hough transform for detecting circles is applied to the preprocessed binarized input image. The transform begins with a large radius which is successively decreased. The resulting circle can be seen in Fig. 2 (b).

Detection of Parapapillary Atrophy. The detection of the papillary atrophy is based on the search for bright areas. Again, the preprocessed input image is binarized and the resulting regions are investigated. Since differences in illumination have been corrected, a global threshold, valid for all images, can be used. The existence of the papillary atrophy can be verified by testing the number and the size of the resulting regions in the binary image and by verifying the success of the Hough transform which is again used for finding a circle in the given set of points. An example of the result of this step is given in Fig. 2 (c).

Contour Point Detection. After three different search spaces have been identified, the different constraints are used all together to restrict the position of valid contour points. The position of valid candidates for the contour line are shown in Fig. 2 (d).

3.3 Fine Segmentation of the External Margin of the Optic Disc

Up to now the detected contour points are unsorted, isolated and not connected. To find a unique object boundary the possible optic disc margin is limited to an Active Contour Model. The final contour can be found by balancing internal and external forces. Internal forces control the elasticity and rigidity of the initial curve resulting from the previous step whereas external forces attract the contour to pixels with some desirable features. For that we used a modified Active Contours model called anchored snakes. The best image points to which the

Fig. 3. Results. Comparison of automated (solid) and manual segmentation (dashed), field of view (fov): 10°× 10° (a); Comparison of segmentation for the same eye captured with two different fov: 10°× 10° (b) and 15°× 15° (c); Result for fov of 20°× 20° (d)

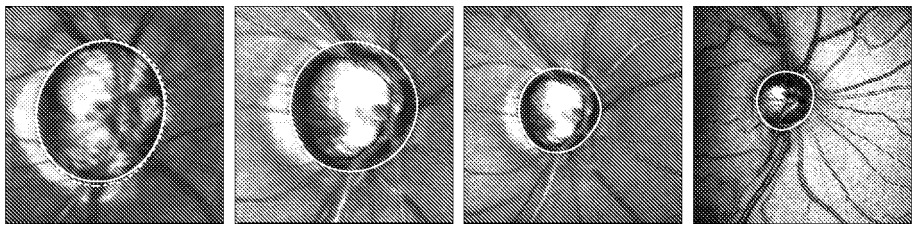

(a) (b) (c) (d)

initial curve should be attracted are searched and set as anchors. Now a spring connection is established between each contour point and the anchors and the forces are balanced [2].

4 Statistical Evaluation of the Algorithm

Data. The study population consists of a subset of a case-control study [3] with known glaucoma diagnosis, control group: $n = 77$, age 56 $(52 - 61)$ years; case group: $n = 82$, age 56 $(51 - 61)$ years (median, 25% and 75% quantile). The data is part of the *Erlangen Glaucoma Registry*. The standard HRT-parameters are used as features for discriminating between normal and glaucomatous eyes. By default, 62 shape parameters of the optic nerve head either globally or in 4 predefined sectors of the papilla are computed from each image. For each image from the case-control study the standard parameters based on the manually and automatically outlined disc margin are computed. The classifiers are evaluated for both sets of features.

Classifiers. The performance of three different classifiers to discriminate between normal and glaucomatous eyes is evaluated: Linear discriminant analysis (LDA) [4], classification trees [5], and classification trees with improvement of the results by bootstrap aggregation (BAGGING) [6].

Error Rate Estimation. The bias corrected .632+ bootstrap estimator [7] is used to estimate the classification error, i. e. the proportion of incorrect classified subjects. Each estimator is computed using 50 bootstrap replications.

5 Results and Conclusion

Examples of the automated contour line calculation are given in Fig. 3. The reproducibility is demonstrated by images (b) and (c) where the same eye was captured in different resolutions. The method was evaluated by measuring overlapping areas outlined automatically and manually, by comparing sensitivity and specificity of the HRT classifier based on automated and manual outlining, and by comparing the error rate estimation of three classifiers. In average the area of

the automatically detected disc margin overlaps in 91% with the reference area (manually outlined). The automated method achieves a sensitivity/specifity of 85% / 58% compared with 88% / 66% for manually outlining. The classification error of LDA for the automated determination of the scleral ring (27.7%) is close to the classification error of LDA for the manual determination of the scleral ring (26.8%). When using CTREE the misclassification rate of automatic detected disc margin (25.2%) is slightly higher than of manually drawn outline (22.0%). The classification error of BAGGING is lower when features based on a manually detected disc margin are used (13.4%, automated detection: 22.2%).

The influence of the automated segmented margin on the classification result was evaluated by means of a case-control study. It could be shown that this approach is suitable for automated glaucoma screening even if the estimated error rates for the automatically segmented external margins were slightly higher than for manually outlined external margins. Shape parameters of the optic nerve head for separation between normal eyes and eyes with glaucomatous damage depend on the exact outlining of the contour line. With the described method 72.3% of images were classified correctly (27.7% was the estimated classification error). In combination with new developed classifiers the estimated error rates are at least as low as with manual outlining and use of linear discriminant analysis.

References

1. R. Chrastek, G. Michelson, K. Donath, M. Wolf, and H. Niemann. Vessel Segmentation in Retina Scans. In J. Jan, J. Kozumplik, I. Provaznik, and Z. Szabo, editors, *Analysis of biomedical signals and images, Proc. of 15th Int. EuraSip Conf. EuroConference BIOSIGNAL 2000*, pages 252–254, Brno, 2000.
2. R. Chrastek, M. Wolf, K. Donath, G. Michelson, and H. Niemann. Automated Outlining of the External Margin of the Optic Disk for Early Diagnosis of Glaucoma. In L. T. Shuskova, O. P. Nikitin, L. M. Samsonov, and P. A. Polushin, editors, *Proc. of 5th Int. Conf. on Physics and Radioelectronics in Medicine and Ecology*, pages 16–19, Vladimir, 2002.
3. T. Hothorn and B. Lausen. Bagging tree classifiers for laser scanning images: Data- and simulation-based strategy. *Artificial Intelligence in Medicine*, 27:65–79, 2003.
4. N. V. Swindale, G. Stjepanovic, A. Chin, and F. S. Mikelberg. Automated analysis of normal and glaucomatous optic nerve head topography images. *Investigative Ophthalmology and Visual Science*, 41(7):1730–42, 2000.
5. L. Breiman, J. H. Friedman, R. A. Olshen, and C. J. Stone. *Classification and regression trees.* Wadsworth, California, 1984.
6. L. Breiman. Bagging predictors. *Machine Learning*, 24(2):123–140, 1996.
7. B. Efron and R. Tibshirani. Improvements on Cross-Validation: The .632+ Bootstrap Method. *Journal of the Am. Statistical Association*, 92(438):548–560, 1997.